The cellular basis for parallel neural transmission of a high-frequency stimulus and its low-frequency envelope

Jason W. Middleton*†‡, André Longtin*†, Jan Benda§, and Leonard Maler†

*Department of Physics, University of Ottawa, 150 Louis Pasteur Avenue, Ottawa, ON, Canada K1N 6N5; †Department of Cellular and Molecular Medicine, University of Ottawa, 451 Smyth Road, Ottawa, ON, Canada K1H 8M5; and §Institute for Theoretical Biology, Humboldt University, Invalidenstrasse 43, D-10115 Berlin, Germany

Edited by Masakazu Konishi, California Institute of Technology, Pasadena, CA, and approved August 4, 2006 (received for review May 18, 2006)

Sensory stimuli often have rich temporal and spatial structure. One class of stimuli that are common to visual and auditory systems and, as we show, the electrosensory system are signals that contain power in a narrow range of temporal (or spatial) frequencies. Characteristic of this class of signals is a slower variation in their amplitude, otherwise known as an envelope. There is evidence suggesting that, in the visual cortex, both narrowband stimuli and their envelopes are coded for in separate and parallel streams. The implementation of this parallel transmission is not well understood at the cellular level. We have identified the cellular basis for the parallel transmission of signal and envelope in the electrosensory system: a two-cell network consisting of an interneuron connected to a pyramidal cell by means of a slow synapse. This circuit could, in principle, be implemented in the auditory or visual cortex by the previously identified biophysics of cortical interneurons.

parallel processing | sensory systems | stimulus envelopes

Narrowband signals (i.e., containing power in a narrow range of frequencies) are an important class of naturalistic stimuli for visual and auditory systems and have associated with them a stimulus envelope, a slow, time-varying contrast or modulation of a sinusoidal carrier arising naturally from, for example, interference between two or more sinusoidal oscillations with similar frequencies. Amplitude-modulated signals have no power at the frequencies of the modulation; instead, they have power centered on the carrier frequency with side bands whose structure depends on the frequency content of the modulation or envelope (1). Because the actual signal contains no power at the envelope frequencies, a system that can extract information about the envelope must use nonlinear processing. An asymmetry in the single-neuron input–output transfer, such as rectification (1), will generate power at the envelope frequencies (2, 3). Recent studies show that visual cortical neurons in cats respond to both low spatial frequency signals and the low-frequency spatial envelopes of high-frequency signals and also suggest that information about stimuli and their envelopes take separate and mutually exclusive linear and nonlinear pathways to reach these cortical neurons (4–11). The cellular and network basis of these parallel cortical computations is not, however, understood.

Apteronotus leptorhynchus generates a sinusoidal electric organ discharge (EOD) that produces an electric field around its body. Recent field studies have shown that *A. leptorhynchus* and related species forage in groups (12) (E. W. Tan and E. S. Fortune, personal communication). Although individual *A. leptorhynchus* maintain a stable EOD frequency (13), the species has a frequency range of ≈700–1,000 Hz. Two fish with widely spaced EOD frequencies will generate a high-frequency envelope of their EOD that is referred to as an amplitude modulation (AM) or beat. Additional fish can superimpose a slowly varying contrast on this high-frequency AM (an envelope of the envelope of the EOD) (12) (E. W. Tan and E. S. Fortune, personal communication) (Fig. 1*A*). To avoid confusion, we will henceforth refer to the AM of the EOD as the "stimulus" and the modulation of the AM as the "envelope." Thus, envelopes are a natural component of the electrosensory environment of an aggregation of wave-type electric fish.

Electroreceptors (P units) are sensitive to the AMs induced by conspecifics (communication signals) and project to the electrosensory lateral line lobe (ELL). Here, we study the response of ELL neurons to the envelope of these signals. We demonstrate that a two-cell network consisting of (*i*) a direct P unit synaptic input to a pyramidal (projection) cell and (*ii*) a high-frequency tuned interneuron projecting onto the pyramidal cell by means of slow $GABA_B$-mediated inhibition is responsible for parallel transmission of the AM stimulus (direct input) and the corresponding stimulus envelope (interneuron-mediated input) in separate channels.

Results

P units and ELL pyramidal cells can respond to the wide range of frequencies present in communication and prey signals (14–16). Here, we investigate their response to the low-frequency envelope signals expected to arise during foraging behavior. Because the particular range of EOD frequencies varies considerably in natural fish groupings (12), we chose to mimic the sensory signals present during foraging by using narrow (frequency) band Gaussian noise stimuli. The analytic signal, extracted by means of the Hilbert transform (17), can be used to estimate the envelope of these stimuli (Fig. 1*B*); the mapping of stimulus to envelope is nonlinear (see *Materials and Methods*). A signal that is amplitude-modulated by a 20-Hz bandwidth will have an envelope with power in the 0- to 20-Hz range (Fig. 1*B*). Basilar pyramidal cells (E cells) are high pass in response to global communication-like signals (15, 16) (Fig. 2*A Upper*), and, as expected, these cells also respond well to 20-Hz band-pass noise with center frequencies ranging from 50 to 90 Hz (Fig. 2*A*). To quantify the response to the stimulus, we use the coherence function (see *Materials and Methods*), which is the linear correlation coefficient between stimulus and response (S-R coherence) as a function of frequency. The S-R coherence does not account for signal transfer when there are nonlinear mappings between the stimulus and the spike train response. The presence of nonlinear mappings can be revealed by the R-R coherence. The R-R coherence is the coherence function between two different spike train responses given identical stimuli; discrepancies between S-R coherence and R-R coherence indicate a nonlinear mapping

Author contributions: J.W.M. and L.M. designed research; J.W.M. performed research; J.W.M., A.L., and J.B. contributed new reagents/analytic tools; J.W.M. and L.M. analyzed data; and J.W.M., L.M., and A.L. wrote the paper.

The authors declare no conflict of interest.

This paper was submitted directly (Track II) to the PNAS office.

Abbreviations: AM, amplitude modulation; EOD, electric organ discharge; ELL, electrosensory lateral line lobe; DBP, deep basilar pyramidal; nP, nucleus praeminentialis.

‡To whom correspondence should be addressed. E-mail: jmidd046@uottawa.ca.

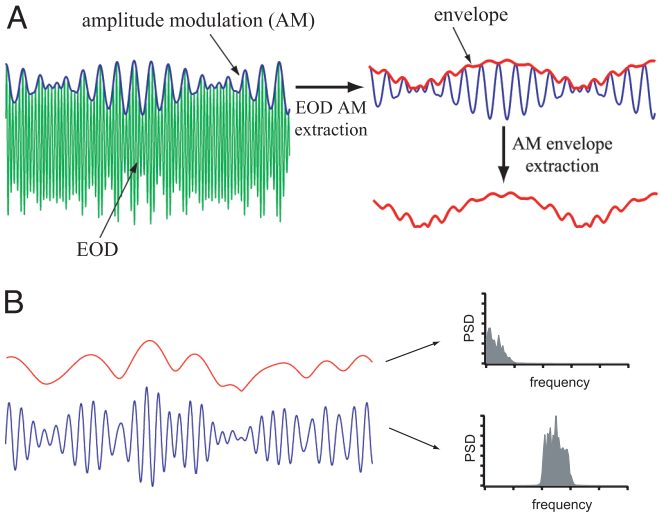

Fig. 1. A mixture of three or more EODs gives rise to narrowband amplitude modulations. (*A*) An example of a fish's EOD mixing with nearby conspecifics with frequency differences of +40 and −50 Hz (green). The AM it creates has a 45-Hz oscillatory component (blue) with a slowly (10 Hz) varying contrast (red). (*B*) To simultaneously test a broad range of EOD frequency differences, we used narrowband Gaussian random AMs with 20-Hz bandwidth and center frequencies ranging from 30 to 90 Hz. This distribution of frequencies is expected based on the EODs of members of foraging groups (12) (E. W. Tan and E. S. Fortune, personal communication). A sample realization of 40- to 60-Hz Gaussian noise (blue) will give an envelope (red) with power in the 0- to 20-Hz range. The respective power spectral densities are shown in *Right*.

(18). For example, the R-R coherence may reveal a response at frequencies not present in the stimulus.

E-R coherence, the coherence between the stimulus envelope and the spike train response, can also be computed. The R-R coherence of E-type pyramidal cells under global stimulus geometry (see *Materials and Methods*) was similar to the S-R coherence over the narrowband stimulus frequency range (in this case, 40–60 Hz; Fig. 2*A*), demonstrating that the signal transfer in this range is linear. However, the R-R coherence also had power in the 0- to 20-Hz range, indicating the presence of a nonlinear transformation, because the signal has no power in that frequency range. Further, at the 0- to 20-Hz range, the E-R coherence was very similar to the R-R coherence, demonstrating that pyramidal cells can respond to the envelope of a complex signal. Because there is no stimulus power in the 0- to 20-Hz range, this response must be due to a nonlinear operation. To quantify the significance of these results, we compared pyramidal cell E-R coherence to that of several other types of upstream neurons, downstream neurons, and interneurons, as well as to the E-R coherence from homogenous Poisson spike trains (as a control) by using a one-way ANOVA; there were highly significant differences across these populations ($P < 10^{-35}$). Multiple comparisons were made (Tukey's honestly significant difference test) to determine the relative response in these different cell types in comparison with Poisson spike trains and each other.

For all classes of pyramidal cells (15) in the centrolateral and lateral segments of the ELL, the E-R coherence, averaged over the 0- to 20-Hz bandwidth, had a mean value (0.29 ± 0.14 SD, $n = 52$ units) that was significantly different from that of homogenous Poisson spike trains (0.01108 ± 10^{-5}; $P < 10^{-3}$). In the following, unless otherwise stated, all significance comparisons are between a Poisson spike train and the cell's response to a global 40- to 60-Hz stimulus.

We then demonstrated that the source of the response to the stimulus envelope does not arise from P unit input to the pyramidal cells or from a nonlinear operation intrinsic to the pyramidal cell. P units are known to respond linearly to a broad range of frequencies of EOD AMs (>200 Hz; data not shown) (16, 19) but, when stimulated by a signal in the 40- to 60-Hz range, they show little E-R coherence (0.034 ± 0.001, $n = 52$; not significant). Stimulation that

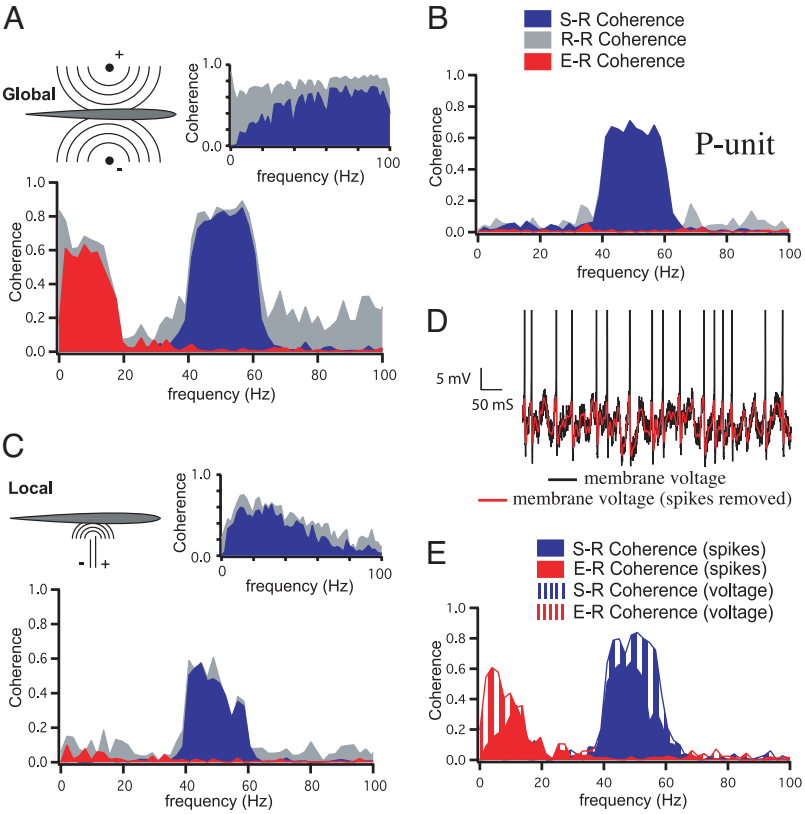

Fig. 2. Pyramidal cells respond to narrowband envelope signals, whereas their afferent inputs do not. (*A*) (*Upper*) In global stimulus geometry, an E-type pyramidal cell, as expected (20), has high-pass filtering characteristics when stimulated with broadband 0- to 100-Hz Gaussian noise. The color coding is according to the legend shown in *B*. (*Lower*) When given narrowband 40- to 60-Hz stimulation, the same pyramidal cell responds linearly to that range of frequencies, shown by the S-R (blue) and R-R (gray) coherences, but it responds nonlinearly to the stimulus envelope, as shown by the R-R (gray) and E-R (red) coherences in the 0- to 20-Hz range. (*B*) Primary sensory afferent fiber (P unit) spike trains are good linear encoders, showing response in the 40- to 60-Hz stimulus range [S-R (blue) and R-R (gray) coherences], yet they show no response to the stimulus envelope. (*C*) (*Upper*) The same pyramidal cell (as in *A*) under spatially local dipole stimulation has low-pass filtering characteristics, as expected (20), when stimulated with 0- to 100-Hz noise. (*Lower*) When given a saturating local 40- to 60-Hz random AM, the cell responds linearly to the input signal, because R-R (gray) and S-R (blue) coherences agree, but not to the stimulus envelope in the 0- to 20-Hz range. (*D*) A sample (E type) pyramidal cell membrane voltage trace (spikes truncated, black) and subthreshold voltage trace (spikes removed, red). (*E*) The S-R and E-R coherences between stimulus and both the spike train and subthreshold membrane voltage for the cell shown in *D*. The S-R and E-R coherences (red and blue, respectively) of the spike train with respect to the stimulus and envelope are shown in solid colors. The S-R and E-R coherences (red and blue, respectively) of the subthreshold voltage with respect to the stimulus and envelope are shown in striped colors. In this case, the spike train coherences were plotted on top of the voltage trace coherences because they have smaller values.

NEUROSCIENCE

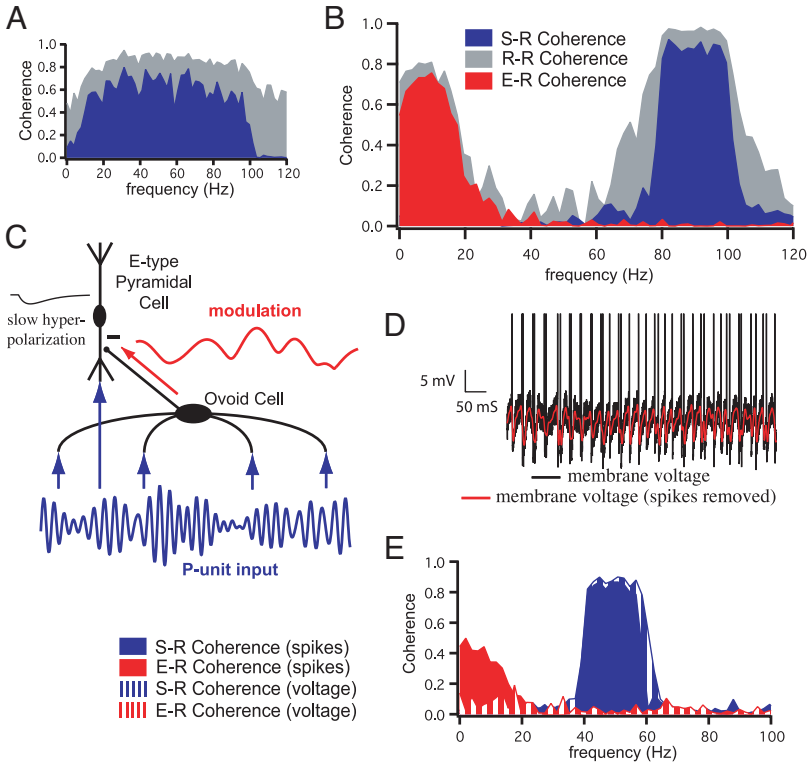

Fig. 3. The spiking mechanism of ovoid cells generates narrowband envelope response that is transmitted to pyramidal cells through slow synapses. (*A*) Ovoid cells are high pass when given global broadband (0–100 Hz shown) Gaussian random AMs. (*B*) In response to global narrowband (80–100 Hz shown; similar results were obtained for center frequencies ranging from 30 to 190 Hz) stimulation, cells respond linearly to the signal (S-R coherence, blue; R-R coherence, gray) and also respond in a nonlinear fashion to the stimulus envelope (R-R coherence, gray; E-R coherence, red) in the 0- to 20-Hz range. (*C*) Under global stimulus geometry, the E-type pyramidal cells receive the stimulus directly through fast glutamatergic synapses from P units (blue arrows), and they receive the stimulus envelope indirectly through $GABA_B$-like synapses from the ovoid cell (red arrow). The ovoid cell is high-frequency tuned so that it will respond well to carrier frequencies, extracting the slower envelope and exclusively passing it to pyramidal cells, filtering out the carrier with a slow synapse. (*D*) A sample voltage trace from a somatic intracellular recording of an ovoid cell (spikes truncated, black). Superposed on this trace is the same trace with spikes removed (see *Materials and Methods*) and low-pass filtered to remove the EOD artifact. The artifact is a small portion of the EOD being picked up directly by the intracellular electrode, which is caused by electrical activity of the cell. (*E*) S-R and E-R coherences between stimulus and both the spike train and subthreshold membrane voltage for the cell shown in *D*. The S-R and E-R coherences (red and blue, respectively) of the spike train with respect to the stimulus and envelope are shown in solid colors. The S-R and E-R coherences (red and blue, respectively) of the subthreshold voltage with respect to the stimulus and envelope are shown in striped colors. In this case, the spike train S-R coherence and the voltage trace E-R coherence were plotted on top because they have smaller values.

saturates only the receptive field center of E-type cells (local stimulus geometry; see *Materials and Methods*) removes the nonlinear effects of the nonclassical receptive field that is present under global stimulation and reveals the isolated processing capabilities of the pyramidal cell (15, 20). Under saturating (20) local stimulus geometry (stimulus intensity matched to the global case), E-type pyramidal cells respond to the 40- to 60-Hz signal yet fail to produce significant E-R coherence (0.026 ± 0.001, $n = 16$; Fig. 2*C*). The direct synaptic input from electroreceptor afferents and the synaptic input from locally projecting interneurons (21) are therefore not able to generate the envelope response.

As a check that the envelope response in the pyramidal cell spike train did not arise from the pyramidal cell spike generation mechanism under global stimulation, we examined the subthreshold membrane potential and calculated both the mean S-R (0.67 ± 0.16, 40- to 60-Hz range, $n = 11$) and E-R (0.42 ± 0.19, 0- to 20-Hz range, $n = 11$) coherence with the stimulus. Fig. 2*D* shows a sample spike train and the subthreshold voltage, low-pass filtered (cut-off of 200 Hz) to remove the EOD artifact (small amplitude potential coming directly from the electric organ), for an E-type pyramidal cell. Fig. 2*E* shows the S-R and E-R coherences between the stimulus and both the spike train and membrane potential. As expected, both responses were greater for membrane potential than the spike train, confirming that the envelope arises from global synaptic inputs to the pyramidal cells and not the spiking nonlinearity.

Given that the source of the envelope to the pyramidal cell is global, we decided to examine ovoid cells, which provide global input to pyramidal cells (21, 22), as a candidate source of their envelope response. As previously reported (23), ovoid cells responded very strongly in a high-pass fashion to broadband global signals (Fig. 3*A*) but not local signals (data not shown); these responses are expected from the anatomy of ovoid cells (21) (i.e., extensive dendritic arborizations receiving P unit inputs from a large fraction of the body surface) (22, 24, 25) and their receipt of gap junction input from P units (25, 26). Ovoid cells also responded strongly to the signal envelope with a mean E-R coherence of 0.58 ± 0.23 (Fig. 3*B*; $n = 11$; $P < 10^{-3}$). Furthermore, unlike pyramidal cells, they also responded to very high-frequency noise signals (up to 180–200 Hz) and exhibited response to envelopes when presented with these stimuli as well (data not shown). Ovoid cells receive only P unit input (27), and, because P units do not themselves extract the envelope, it seemed likely that the envelope must first be extracted by a nonlinearity associated with ovoid cell spiking. Preliminary data suggest that envelope extraction requires low membrane noise and the spiking threshold nonlinearity (J.W.M., E. Harvey-Girard, A.L., and L.M., unpublished work). Most recordings from ovoid cells were made from their thick axons, as previously reported (23), and their membrane potential did not reflect the stimulus (data not shown). In one case, however, we achieved an intracellular somatic recording from an ovoid cell. In this case, the membrane clearly tracked the stimulus (Fig. 3*D*) so that the S-R was very high and similar to that of the spike train (Fig. 3*E*). The membrane potential of this cell showed no E-R coherence, although its spike train clearly did (Fig. 3*E*; average E-R coherence of 0.37 in the 0- to 20-Hz range; average S-R coherence of 0.86 in the 40- to 60-Hz range). This finding suggests that the ovoid cell is the first site where a nonlinearity associated with the spike threshold extracts the signal envelope associated with band-pass Gaussian stimuli.

It appeared puzzling that the strong linear response of ovoid cells to the high-frequency signal was not also transmitted to its pyramidal cell targets. Ovoid cells are GABAergic (21), and their stimulation *in vivo* (23) or *in vitro* (26) causes a slow inhibitory postsynaptic potential (IPSP) in E-type pyramidal cells that appears to be mediated solely by $GABA_B$-like receptors (26). We propose that these slow IPSPs will act as a low-pass filter of the ovoid cell output, removing the high-frequency content and transmitting only its envelope response.

As an additional test of our hypotheses, we also examined envelope extraction in nonbasilar pyramidal cells (I cells). I cells are a morphologically and functionally distinct population that receives indirect P unit input (by means of locally projecting interneurons) and is low pass (15, 22, 27). As expected, these cells responded at

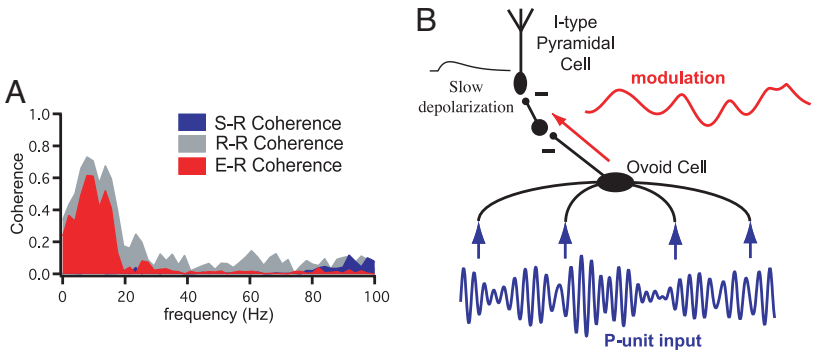

Fig. 4. The envelope response generated by ovoid cells can also be transmitted to principal cells via intermediate interneurons. (*A*) Under global stimulus configuration, some nonbasilar, or I-type, pyramidal cells fail to respond to the AM signal but show strong response to the stimulus envelope as shown by the R-R (gray) and E-R (red) coherences in the 0- to 20-Hz range. (*B*) The response in I-type cells is mediated by an additional inverting local interneuron, showing that the envelope response may be hyperpolarizing or depolarizing in nature.

best weakly to a global band-pass signal when its center frequency was >30 Hz; however, they still produced E-R coherence comparable to that of E cells. This response is illustrated in Fig. 4*A*, where an I cell given 80- to 100-Hz stimulation showed no response to the signal but still responded to its envelope (E-R, 0.20 ± 0.09; S-R, 0.029 ± 0.021; $n = 8$; Fig. 4*A*). We conclude that the I-type pyramidal cell is not responsible for generating the envelope response; it shows no response to the narrowband signal from which to extract the envelope (4, 28). This form of processing is similar to neurons in the visual or auditory systems showing no linear response to a high-frequency signal and instead responding to its envelope (4–6, 8–10, 29–33). Extraction of the signal envelope is therefore not due to the intrinsic dynamics of pyramidal cells or input from electroreceptors (directly or by means of local granular interneurons). With these sources eliminated, we conclude that the envelope response requires input with global stimulus geometry, presumably the ovoid cell (see *Materials and Methods*).

Ovoid cells project indirectly to I-type pyramidal cells by means of local granular interneurons (21), and the resulting responses are also slow (23); because the ovoid cell input to I cells is by means of an inhibitory interneuron, it is sign-inverted and appears as a slow depolarizing potential (23). Thus, we propose that the envelope response of I-type pyramidal cells is also generated by the ovoid cells but by means of slow modulation of the response of local interneurons (23, 26).

Our model for the parallel transmission of the envelope along with the signal to E-type ELL pyramidal cells is illustrated in Fig. 3*C*. Ovoid cells respond to the high-frequency signals and generate a response to its envelope by means of a nonlinearity, such as half-wave rectification (1), possibly implemented by the thresholding spiking nonlinearity (34); they transmit the response to the stimulus envelope to the pyramidal cells by means of a slow synapse, and information about the stimulus (to E cells) comes by means of fast glutamatergic P unit synapse on their basilar bush (26). Fig. 4*B* shows a model to explain the I cell envelope response: The ovoid cell passes on the envelope signal to another local interneuron, with the net result being depolarization at the I-type pyramidal cell. Because, for a narrowband stimulus, the envelope is the same whether or not the stimulus is inverted, it does not matter whether the slow signal is passed by means of inhibitory or excitatory synaptic input, as long as there is a slow time course.

In addition to the ovoid cell global feedforward input, the ELL pyramidal cells receive extensive global feedback input (15, 35), and the envelope response might therefore also be generated or modified by means of a feedback mechanism. Feedback input to the ELL emanates mainly and perhaps exclusively from one class of pyramidal cells: the deep basilar pyramidal (DBP) cells (35). Previous studies have shown that DBP cells fail to respond to very high-frequency AMs (15). However, global stimulation of DBP cells with 180- to 200-Hz stimuli generated an envelope response without any response (S-R or R-R) to the signal itself (E-R, 0.17 ± 0.07; S-R, 0.006 ± 0.002; $n = 5$, Fig. 5*A*). Ovoid cells are the only ELL neurons able to respond to AMs with frequencies >180 Hz (data not shown); they are therefore the sole source of DBP cell input capable of generating envelope power.

Furthermore, under these conditions, there should be no source of narrowband, high-frequency (>180 Hz) input available to higher brain feedback circuitry from which to extract the envelope. To investigate whether the global feedback pathway driven by the DBP cells (35) might still influence the envelope response of pyramidal cells, we have recorded activity from feedback afferent fibers from the nucleus praeminentialis (nP) in the eminentia granularis posterioris, a cerebellar-like structure shown to be responsible for global gain control and adaptive sensory cancellation (35). Consistent with earlier reports (35), we found that nP afferents were high pass (Fig. 5*B Inset*) and also responded well to narrowband frequencies. These afferents did not, however, respond to the envelope in their spike train response, having a mean E-R coherence of 0.049 ± 0.001 (Fig. 5*B*; $n = 16$; not significant). It is therefore unlikely that feedback input contributes to or modifies the pyramidal cells' envelope response. Because the DBP cells did respond to the stimulus envelope but nP afferents did not, these results imply

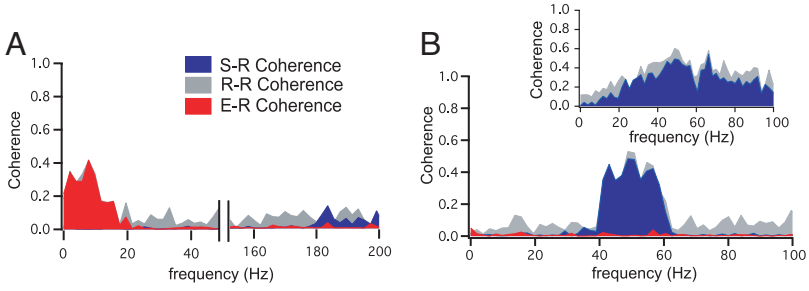

Fig. 5. Feedback inputs are not responsible for generating the envelope response. (*A*) When given high-frequency global stimulation outside of their range of sensitivity (180–200 Hz shown), DBP cells, the sole source of inputs to higher feedback centers (15), show envelope response (R-R coherence, gray; E-R coherence, red) in the 0- to 20-Hz range but show no response in the 180- to 200-Hz range. This lack of response also rules out the role of feedback pathways in the generation of the stimulus envelope to the pyramidal cells because, for the neurons responsible for the feedback signal, the narrowband signal is unavailable (blue) for the extraction of the envelope under this stimulus condition. (*B*) (*Inset*) The majority of nP afferent axons in the eminentia granularis posterioris are high pass in response to broadband 0- to 100-Hz stimulation. When given narrowband high-frequency (80–100 Hz shown; similar results were obtained for center frequencies ranging from 30 to 90 Hz) stimulation, the spike trains show good response to the direct stimulus (S-R coherence, blue; R-R coherence, red) and no response to the envelope. This finding rules out the transmission of the envelope signal to the pyramidal cell apical dendrite through the indirect feedback pathway.

NEUROSCIENCE

that the envelope response is filtered out within nP and, unlike direct low-frequency input (14, 20, 35), is not available as a cancellation signal to the ELL.

The E-R coherences (global stimulation) of E- and I-type pyramidal cells were not significantly different ($P = 0.1482$), so the responses of these populations were pooled. The E-R coherence of pyramidal cells is significantly greater than P units, pyramidal cells with local stimulation, and nP afferents ($P < 10^{-3}$). The E-R coherences of these last three populations were not significantly different from each other or from the Poisson spike train. The mean E-R coherence of the ovoid cells is about double that of pyramidal cells (0.58 vs. 0.29; $P < 10^{-5}$), further suggesting that the ovoid cells are the source of envelope response in pyramidal cells.

Discussion

We have shown that parallel pathways transmit the electrosensory narrowband signal and their envelopes from P unit electroreceptors to pyramidal cells. The direct projection from P units to pyramidal cells conveys the narrowband signal. An indirect pathway from P units to pyramidal cells by means of a fast interneuron with slow output synaptic kinetics extracts the envelope of the narrowband signal.

Similar processes may be operative in the auditory and visual system. The spectrotemporal structure of communication vocalizations reveals modulations at different carrier frequencies (36, 37). The relationship between envelope and carrier frequencies determines the perception of pitch fluctuation, pitch roughness, and subharmonic or residue pitches (2, 38, 39). In visual scenes, envelopes (spatial contrast modulations) are responsible for groupings of objects and illusory contour perception (5, 7, 8). There is mounting evidence that the invariant response to object groupings arises from a parallel network structure consisting of separate linear (first order) and nonlinear (higher order) channels. This parallel transmission supports the idea of cue invariance in the visual system, where objects are perceived similarly if they are delineated by either intensity or contrast boundaries (4–10). It has also been shown that cells in the inferior colliculus respond to interaural time differences of low-frequency pure tones and low-frequency modulations of high-frequency carrier tones (30, 33). This response to low-frequency signals and envelopes of high-frequency narrowband signals can be thought of as another form of cue invariance, except in this case, it pertains to sound localization, not object perception. Observations of independence between optimal carrier and envelope frequencies in the auditory cortex also support the idea of parallel transmission of signal and envelope (29, 31, 32).

Electric fish may require separate responses to both the envelope and direct electrosensory signals to distinguish the frequencies, and therefore the identities, of the other fish within a foraging group. EOD frequency differences between fish are detected as direct inputs to the ELL. At very high EOD frequency differences (>200 Hz), the P units and thus the pyramidal cells can no longer reliably track the stimulus (unpublished data); furthermore, midbrain neurons in receipt of ELL input respond mostly to lower frequencies in a related wave-type gymnotiform fish (40).

In auditory and visual systems, it is observed that the envelope-generating mechanism does not interfere with response to direct, low-frequency stimulation (4–6, 8–10, 29–33). In fact, when first-order and higher order stimuli represent the same cues, they can actually interact constructively, as was recently shown in stereopsis (11). The magnitude of response to envelopes depends on the carrier frequency, which is typically much higher than envelope frequencies. A result of this design is that information typically takes one of two parallel pathways (i.e., linear or nonlinear). The direct P unit synapses onto pyramidal cells (linear) in parallel with the ovoid cell synaptic input to pyramidal cells (nonlinear) satisfies this design criteria (Fig. 3*D*). A low-frequency signal delivered to the cell's receptive field center will pass through the P unit synapses to the pyramidal cell (linear pathway; Fig. 2*C Upper*) but will be filtered out in the ovoid cell because of its high-pass frequency response (Fig. 3*A*). In contrast, ovoid cells respond to even very high-frequency narrowband signals (180–200 Hz; data not shown), extracting the low-frequency envelope and passing to the pyramidal cell (nonlinear pathway); I-type pyramidal cells have a low-pass frequency response (15) and thus do not respond directly to the very high-frequency signals.

The two-cell network we have identified, consisting of a high-pass interneuron that can extract the envelope and that connects to the output cells by means of slow inhibitory synapses, is a simple way of extracting and separately transmitting linear and nonlinear (slower) stimulus features. The types of stimuli used in this study are relevant to visual and auditory systems as well (2, 5, 8, 36, 37, 39). Response to the signal envelope is seen up to cortical levels of both auditory and visual systems. The basic building blocks of our simple network, high-pass interneurons (41) and interneurons that use $GABA_B$ receptors on pyramidal cells (42–45), are present at cortical levels, suggesting that this simple neural implementation of parallel linear and nonlinear information streams might be widespread.

Materials and Methods

Electrophysiological Recording. Data from 32 adult *A. leptorhynchus* were used in this study. For surgical exposure of the ELL, fish were anesthetized (with Tricaine-S; Western Chemical, Ferndale, WA). After surgery, fish were immobilized (with pancuronium bromide; Sabex, Boucherville, QC, Canada) and transferred to a tank (28°C) where they were respired by a constant flow of oxygenated water through their mouth. Intracellular and extracellular recordings from ELL neurons and axons were routinely made with borosilicate microelectrodes (70–140 megaohms) filled with 3 M KAc (for intracellular recordings) or tungsten wire electrodes (for extracellular recordings; TM33C10; WPI, Saratosa, FL); the recording electrodes were advanced into the ELL with a piezoelectric microdrive (Inchworm, IW-711; Burleigh, Fishers, NY). Electroreceptor afferents (P units), pyramidal cells, one class of ELL interneurons (ovoid cells), and feedback inputs to the ELL were identified based on electrode depth, baseline discharge statistics, and responses to step changes in the EOD amplitude and sinusoidal and random EOD AMs; these responses are well characterized and successfully discriminate cell types (23, 24, 35, 46). Recorded signals were amplified with an Axoprobe, (Axon Instruments, Union City, CA; for intracellular recordings, $n = 43$; for extracellular recordings, $n = 9$) and stored on a desktop personal computer. Analysis was performed offline by using MATLAB software (MathWorks, Natick, MA). All experimental and surgical protocols were approved by the University of Ottawa Animal Care Committee.

The EOD unperturbed by the stimulus was recorded between the head and tail of the fish by using two vertical carbon rods (11 cm long and 8 mm in diameter). Two chloridized silver wires, insulted except at the tips and spaced 2 mm apart, were placed ≈1 mm away from, and at right angles to, the fish's body; these electrodes were used to record the stimulus-induced EOD AMs.

The membrane potentials, the unperturbed EOD, the modulated EOD transverse to the fish, and the attenuated stimulus were digitized at 20 kHz with a MultiIO board (PCI-MIO-16E-4; National Instruments, Austin, TX) on an Intel Pentium IV 1.8-GHz Linux personal computer. Spike and EOD detection, stimulus generation and attenuation, and preanalysis of the data were performed online during the experiment with Online Electrophysiology Laboratory (OEL) software (47).

Stimulation. AMs of the EOD were created by sampling the head–tail carbon electrodes and multiplying this EOD with the desired modulation. This signal was delivered in phase with the fish's own EOD by means of stimulation electrodes placed over the cells' receptive field center (local geometry) or across the fish's body (global geometry) as described in refs. 20, 48, and 49. The

output of the stimulation electrodes was attenuated so that, when combined with the fish's own EOD, the correct signal contrast was produced. The stimulation electrodes in global geometry consisted of two carbon rods (20 cm long and 8 mm in diameter) parallel to the rostrocaudal axis placed on either side 10 cm away. In local stimulus geometry, two thin tungsten wires, insulated except at the tips, with a spacing of 2 mm were placed 5 mm away from the surface of the fish perpendicular to the body axis.

There were two classes of stimuli used: broadband and narrowband Gaussian distributed noise. Both were derived from Gaussian white noise by applying a low-pass filter (100-Hz cut-off frequency) or a band-pass filter (20-Hz bandwidth with center frequencies ranging from 30 to 290 Hz), respectively. Narrowband signals are a convenient representation of the types of signals that electric fish would see while aggregating with a population of conspecifics. Wave-type weakly electric fish have a natural distribution of EOD frequencies (12). In a population of three or more, the types of EOD modulations they would experience would be neither broadband nor pure tones; therefore, we chose narrowband Gaussian noise as a mimic of this kind of electrosensory signal.

Extracting the Stimulus Envelope. The Hilbert transform is a useful tool in the analysis of time-varying stationary signals with oscillatory components. A harmonic oscillation, $x(t)$, can be represented geometrically as a limit cycle in the complex plane by creating the analytic signal, $z(t) = x(t) + iy(t)$, whose imaginary part is composed of the real frequency components phase-shifted by 90° [i.e., $y(t) = H[x](t)$], where H is the Hilbert transform:

$$H[x](t) = \frac{1}{\pi} P \int_{-\infty}^{\infty} \frac{x(\tau)}{t - \tau} d\tau. \quad [1]$$

In the case of the narrowband signals that we used, the radial component of the corresponding analytic signal has an intuitive interpretation. The radial component,

$$A(t) = \sqrt{x^2(t) + y^2(t)}, \quad [2]$$

represents the instantaneous amplitude or signal envelope that arises because of interference of spectral components of the signal having similar frequencies.

Data Analysis. The coherence between two stationary signals, $x(t)$ and $y(t)$, is defined as

$$C_{XY}(f) = \frac{|S_{XY}(f)|^2}{S_{XX}(f) S_{YY}(f)}, \quad [3]$$

where $S_{XY}(f)$ is the cross-spectral density between x and y and S_{XX} and S_{YY} are the autospectral densities of x and y, respectively. It measures the correlations of phase and amplitude of oscillations between the two signals as a function of their frequency. The coherence gives a measure of the filtering properties of a transfer system if $x(t)$ and $y(t)$ refer to the input and output. We are interested in the response, $R(t)$, of a given neuron in the form of an action potential sequence or spike train to a given stimulus, $S(t)$, at the sensory periphery. The spike train response can be defined mathematically as a series of delta functions centered at the spike times: $R(t) = \sum_i \delta(t - t_i)$. We use the notation $C_{SR}(f)$, or, equivalently, S-R coherence, to refer to the coherence between stimulus and response in the form of a spike train. We also use the notation S-R coherence to denote the response between subthreshold membrane voltage and the stimulus, but we explicitly state the form of response where used. The coherence between two responses to the same signal is denoted $C_{RR}(f)$, and, in general, the inequality $C_{SR}(f) \leq \sqrt{C_{RR}(f)}$ holds, so that the responses are at least linearly related to one another by means of the stimulus (18); the stimulus–response and response–response coherences are lower (linear) and upper bounds, respectively, on the information that can be transmitted by a neuron about a signal (18). Throughout, we compare S-R coherence to the square root of R-R coherence but denote it as simply R-R coherence, for brevity. A more formal connection to mutual information has been established by using these measures but is not used here (50). The notation E-R coherence is used to represent the response of the spike train (or subthreshold voltage, where stated) to the stimulus envelope calculated by means of the Hilbert transform. The subthreshold membrane voltage was obtained from the intracellular voltage recording by using a spike removal algorithm. This algorithm detected spikes by using voltage and voltage derivative threshold conditions, and it removed them by replacing the voltage trajectory during a spike by the average of the values immediately before and after the spike. Significance of coherence responses in the populations of different cells was done by comparison to a numerically simulated Poisson spike train with a firing rate equal to the average rate of E-type pyramidal cells. A one-way ANOVA was performed between the distribution of average coherence values in the stimulus bandwidth and the envelope bandwidth and the distribution of coherence values in the respective bandwidths from the Poisson spike trains.

1. Rice SO (1954) *Mathematical Analysis of Random Noise* (Dover, New York).
2. Burns EM, Viemeister NF (1976) *J Acoust Soc Am* 60:863–869.
3. Viemeister NF (1979) *J Acoust Soc Am* 66:1364–1380.
4. Baker CL, Jr (1999) *Curr Opin Neurobiol* 9:461–466.
5. Grosof DH, Shapley RM, Hawken MJ (1993) *Nature* 365:550–552.
6. Mareschal I, Baker CL, Jr (1998) *Nat Neurosci* 1:150–154.
7. McGraw PV, Levi DM, Whitaker D (1999) *Nat Neurosci* 2:479–484.
8. Shapley R (1998) *Nat Neurosci* 1:95–96.
9. Zhou YX, Baker CL, Jr (1993) *Science* 261:98–101.
10. Zhou YX, Baker CL, Jr (1996) *J Neurophysiol* 75:1038–1050.
11. Tanaka H, Ohzawa I (2006) *J Neurosci* 26:4370–4382.
12. Tan EW, Nizar JM, Carrera GE, Fortune ES (2005) *Behav Brain Res* 164:83–92.
13. Moortgat KT, Keller CH, Bullock TH, Sejnowski TJ (1998) *Proc Natl Acad Sci USA* 95:4684–4689.
14. Bastian J, Chacron MJ, Maler L (2004) *Neuron* 41:767–779.
15. Chacron MJ, Maler L, Bastian J (2005) *J Neurosci* 25:5521–5532.
16. Chacron MJ, Maler L, Bastian J (2005) *Nat Neurosci* 8:673–678.
17. Oppenheim AV, Schafer RW (1999) *Discrete Time Signal Processing* (Prentice–Hall, Upper Saddle River, NJ).
18. Roddey JC, Girish B, Miller JP (2000) *J Comput Neurosci* 8:95–112.
19. Wessel R, Koch C, Gabbiani F (1996) *J Neurophysiol* 75:2280–2293.
20. Chacron MJ, Doiron B, Maler L, Longtin A, Bastian J (2003) *Nature* 423:77–81.
21. Maler L, Mugnaini E (1994) *J Comp Neurol* 345:224–252.
22. Maler L (1979) *J Comp Neurol* 183:323–363.
23. Bastian J, Courtright J, Crawford J (1993) *J Comp Physiol A* 173:257–274.
24. Bastian J, Courtright J (1991) *J Comp Physiol A* 168:393–407.
25. Yamamoto T, Maler L, Hertzberg EL, Nagy JI (1989) *J Comp Neurol* 289:509–536.
26. Berman NJ, Maler L (1998) *J Neurophysiol* 80:3173–3196.
27. Maler L, Sas EK, Rogers J (1981) *J Comp Neurol* 195:87–139.
28. Demb JB, Zaghloul K, Sterling P (2001) *Neuron* 32:711–721.
29. Eggermont JJ (1998) *J Neurophysiol* 80:2743–2764.
30. Griffin SJ, Bernstein LR, Ingham NJ, McAlpine D (2005) *J Neurophysiol* 93:3463–3478.
31. Liang L, Lu T, Wang X (2002) *J Neurophysiol* 87:2237–2261.
32. Schreiner CE, Urbas JV (1988) *Hear Res* 32:49–63.
33. Shackleton TM, Skottun BC, Arnott RH, Palmer AR (2003) *J Neurosci* 23:716–724.
34. Chialvo DR (2003) *Chaos* 13:1226–1230.
35. Bastian J, Bratton B (1990) *J Neurosci* 10:1226–1240.
36. Attias H, Schreiner CE (1999) *Low-Order Temporal Statistics of Natural Sounds* (MIT Press, Cambridge, MA).
37. Nelken I, Rotman Y, Bar Yosef O (1999) *Nature* 397:154–157.
38. Burns EM, Viemeister NF (1981) *J Acoust Soc Am* 70:1655–1660.
39. Schouten JF, Ritsma RJ, Cardozo BL (1962) *J Acoust Soc Am* 34:1418–1424.
40. Rose GJ, Etter N, Alder TB (1994) *J Neurosci* 175:467–474.
41. Hasenstaub A, Shu Y, Haider B, Kraushaar U, Duque A, McCormick DA (2005) *Neuron* 47:423–435.
42. Benardo LS (1994) *J Physiol* 476:203–215.
43. Shao Z, Burkhalter A (1999) *J Neurophysiol* 81:1014–1024.
44. Tamas G, Lorincz A, Simon A, Szabadics J (2003) *Science* 299:1902–1905.
45. Thomson AM, Destexhe A (1999) *Neuroscience* 92:1193–1215.
46. Saunders J, Bastian J (1984) *J Comp Physiol A* 154:199–209.
47. Benda J, Longtin A, Maler L (2005) *J Neurosci* 25:2312–2321.
48. Bastian J, Chacron MJ, Maler L (2002) *J Neurosci* 22:4577–4590.
49. Doiron B, Lindner B, Longtin A, Maler L, Bastian J (2004) *Phys Rev Lett* 93:048101.
50. Borst A, Theunissen FE (1999) *Nat Neurosci* 2:947–957.